CHAPTER 9

Identification of potential inhibitors against Human Lemur Tyrosine Kinase-3 (LMTK3) domain: An E-pharmacophore approach

Identification of potential inhibitors against Human Lemur Tyrosine Kinase-3 (LMTK3) domain: An E-pharmacophore approach

9.1 Abstract

Since LMTK3 is considered to be a new oncogenic target, there is a need to identify potential inhibitors. The discovery of specific and selective ATP competitive inhibitors remains a major challenge due to the conserved nature of kinase domain. We made an attempt to screen probable non-ATP competitive LMTK3 inhibitors from the Asinex database using Schrodinger drug design suite by submitting the modelled and well equilibrated 3-D structure of LMTK3 domain. Based on the Glide XP docking score, the top three hits (BAS12945106, BDF24025570, BAS01313675) for LMTK3 were identified. And these compounds observed to bind to LMTK3 domain, at a region distinct from the ATP binding pocket. We considered these hits to be the probable Type IV kinase inhibitor for LMTK3. The top three LMTK3-hit complexes were found to be stable from the RMSD and Radius of gyration analysis. From MM-PBSA analysis, we noticed the top three hits to exhibit high binding affinity for the LMTK3 domain. And from the PMF results, we observed, among the three hits, BAS01313675 have higher dissociation energy barrier. From the binding modes of LMTK3-hit complexes, an energy optimized (E) pharmacophoric features were generated for the LMTK3 inhibitor. Our resulting E-pharmacophore model for the LMTK3 inhibitor contained two aromatic rings, a hydrogen bond donor, and a hydrogen bond acceptor sites. Our findings may be helpful in the development of new potential LMTK3 inhibitors for effective breast cancer therapeutics.

9.2. Introduction

The discovery of selective ATP competitive inhibitors remains as a major challenge [456]. Therefore, targeting less conserved allosteric sites of the kinases have been an active area of research for high selectivity [457, 458]. In the present study, we made an attempt to identify potential inhibitors against LMTK3 through energy optimized (E) pharmacophore modeling approach using structure guided high throughput virtual

screening in Schrodinger drug discovery suite [279]. This method has been used in the recent days to identify potential inhibitors for various diseases [459-463]. Schrodinger drug discovery suite implement high throughput virtual screening (HTVS), standard precision docking (SP) and extra precision docking (XP) [464], using this hierarchical screening protocol, Asinex small molecular database was screened against LMTK3 domain. Based on the Glide XP score, we selected three top hits (BAS12945106, BDF24025570, BAS01313675). Based on the Glide XP docking score and the binding mode of the top hits with LMTK3, the E-pharmacophore model was generated. Binding mode analysis of all the three hits with LMTK3 domain, revealed that the hits were bound to the site remote from the ATP binding pocket, which could act as a possible allosteric inhibitors of LMTK3. Further RMSD and Rg analysis and Molecular Mechanics Poisson-Boltzmann surface area continuum solvation (MM-PBSA) binding free energy calculation [186,351] revealed the stability of the complexes in the dynamic system. In addition, per residue energy decomposition analysis for interacting residues of LMTK3 domain with the hits were found to have favorable energy contributions and results supported the high binding affinity of the three hits with LMTK3 domain. From the free energy calculation we observed that among the three hits, compound BAS01313675 has the highest total binding free energy and ensuring to be the best E-pharmacophore model, which may be essential for the inhibition of LMTK3. Our resulting pharmacophore model contained two aromatic rings, a hydrogen bond acceptor and a hydrogen bond donor sites. Our findings from the combined structure guided drug design approach surely broaden the knowledge, and will help the medicinal chemist in the identification of potential novel drug candidates against LMTK3, which could be effective in breast cancer therapeutics.

9.3. Materials and Methods

9.3.1. Structural Modeling and validation

The protein sequence of human LMTK3 (1486 amino acids) was retrieved from the UniprotKB [296] database (accession no: AOAOAOMQW5). We modeled $LMTK3_{162-440}$ domain from I-TASSER [99]. According to the CASP ranking, I-TASSER has been reported to be the best automated protein prediction server. The best model was

identified based on the C-score calculated from the relative clustering structural density and consensus significance. Template modelling (TM) score and root mean square deviation (RMSD) are used to evaluate the accuracy of the best model. Then the modeled structure of $LMTK3_{162-440}$ was validated by the ProSA server [300], verify 3D [301,302], and the RAMPAGE server [303].

9.3.2. Molecular dynamics simulation of Apo- LMTK3 domain

The modelled structure of LMTK3 was subjected to MD simulation. To perform MD simulation, we used Particle Mesh Ewald molecular dynamics (PMEMD) [305] algorithm from AMBER14 software package [465]. AMBER ff99SB force field [306] protein parameters were applied on LMTK3. Using xleap module of AMBER14, the modelled LMTK3 domain was solvated using TIP3P [167] water model with the water box of size 10 Å from the solute in the x, y, and z coordinates, followed by the addition of three sodium counter-ions to neutralize the protein charge. The topology and coordinate files were prepared for the solvated system.

Next, we performed energy minimization, wherein we reduced the potential energy of the initial structure using 1000 steps of the steepest descent algorithm, followed by 1000 steps of the conjugate gradient method. During the energy minimization, we fixed the protein molecule using harmonic constraints (excluding the water molecules) with a force constant of 30 kcal mol^{-1} $Å^2$ to overcome the bad contacts between water molecules and the protein. The subsequent minimization was carried out without any constraints for 2000 cycles (1000 cycle of steepest descent and 1000 cycle of conjugate gradient). The system was slowly heated from 0 to 300 K with a weak 20 kcal mol^{-1} $Å^{-2}$ constraints at 40 ps in NVT condition. This allows the structure to undergo slow relaxation. Using a geometrical tolerances of 5×10^{-4} Å, the SHAKE [165] constraints were imposed on all covalent bonds involving hydrogen atoms with a time step of 2 fs. The equilibration and the long range production steps were performed in NPT condition (T=300 K and P=1atm), where the temperature regulation was achieved using the Berendsen weak coupling method [166] (0.5 ps time constant for heat bath coupling and 0.2 ps pressure relaxation time). Finally, conformational dynamics of LMTK3 domain was carried out upto 21 ns in NPT condition using a heat bath coupling time

constant of 1 ns. The analysis of structural convergence properties, such as Root Mean Square Deviation (RMSD), Radius of gyration (Rg), and Root Mean Square Fluctuation (RMSF) were carried out using cpptraj algorithm [358]. For the 3D visualization of the molecule, we used UCSF Chimera [180] and VMD [179]. We further extracted the lowest energy conformer of LMTK3 domain from the MD trajectories in order to design an E-Pharmacophore model.

9.3.3 Steps for E-Pharmacophore model generation

9.3.3.1 Protein preparation

The protein preparation wizard in Maestro 9.0.111 (Maestro v 9.0.111 Schrodinger LLC, New York, NY) [279] which comes along with the Schrodinger suite was used to prepare the protein (LMTK3) that was extracted from the MD trajectories. This protein preparation step includes the determination of the optimal protonation states for the histidine residues, correcting potentially transposed heavy atoms in arginine, glutamine and histidine side chains, and the optimization of the protein's hydrogen bond network. The protein is later minimized with the restraints using the OPLS 2005 (optimized potential for liquid simulations 2005) force field [280].

9.3.3.2 Receptor Grid Generation

The protein prepared in the earlier step was loaded into Schrodinger Maestro for the generation of the receptor grid for molecular docking. It was generated using the receptor grid generation wizard in the Schrodinger suite. In order to check the affinity of the database compounds for the binding site (Asn320, Leu 316, Arg249, Asp246, Gln243, Val191, Leu 331), the size of the grid box was adjusted such that it accompanied the entire binding site; the grid box was centered on to the binding site.

9.3.3.3. Small molecular library preparation

The commercial chemical database, Asinex that houses the library of over 3,00,000 small molecules, was processed with tough redundancy checking and Lipinski filters to select compounds that have better druggability. The database compounds were prepared using the Ligprep program (LigPrep, version 2.5, Schrodinger, LLC, New York, NY,

2011). This program generates the ligands based on the variations in their ionization states, wide pH ranges 5-9, combinations of stereoisomers, and tautomers [281].

9.3.3.4. High throughput Virtual Screening (HTVS)

The processed compounds were subjected to high throughput virtual screening protocol using the Glide docking algorithm implemented in Maestro 9.2V. The Glide scoring is done based on the Chem Score function of Eldridge and group [282], which identifies various types of interactions likes hydrophobic interaction, stable hydrogen bonding and metal-ligation interactions, and restricts any type of steric interactions. This hierarchical screening approach includes high throughput virtual screening (HTVS), standard precision docking (SP) and extra precision docking (XP). The prepared compounds were initially screened using HTVS algorithm, and then the top 1000 hits were subjected for Glide SP, and finally the best 100 compounds were subjected for Glide XP docking against LMTK3. Glide XP (grid based ligand docking with energetic, extra precision) algorithm approximates a systematic search of positions, conformations and orientations of the ligands, eliminating the unwanted conformations using scoring via a series of hierarchical filters. We obtained three top hits (BAS12945106, BDF24025570, BAS01313675) bound to LMTK3 domain with good Glide XP score.

9.3.3.5. Energy Optimized (E)-Pharmacophore model generation

Energy-based pharmacophoric features are generated by considering the default chemical features such as hydrogen bond acceptor (A), donor (D), hydrophobic (H), negative (N), positive (P), and aromatic ring (R). The Glide scoring terms were computed and energies were mapped onto the atom [283]. Each pharmacophoric feature is first assigned with an energetic value which is equal to the sum of the Glide XP contributions made by all the atoms present in that site. Based on the energetic terms used in the Glide XP descriptors, the sites are quantified and ranked. The best four pharmacophoric features were selected for potential inhibition of LMTK3, based on the Glide XP score.

9.3.4. Molecular dynamics (MD) simulation of the LMTK3-hit complexes

All of the three complex systems were subjected to MD using the Particle Mesh Ewald molecular dynamics (PMEMD) module of AMBER14 software package. The partial charges and force field parameters for all the three compounds were generated automatically using the Antechamber program implemented in AMBER14. The force field parameters were given for the ligand and the protein using the xleap module in AMBER14. General Amber force field (GAFF) [161] and AM1-BCC [466] charges were used for the ligands, while AMBER ff99SB force field [306] was used for the protein (LMTK3). Topology and coordinate files for the entire complex systems were then generated using the xleap program of AMBER14. The resultant initial complex systems were solvated in a rectangular periodic TIP3P box [167], having size of 10 Å from the solute in the x, y, and z coordinates and sodium counter-ions were added to neutralize the complex systems. The complex systems were then energy minimized, temperature and pressure equilibrated according to the same parameters mentioned previously under sub-section 9.3.2. Finally, NPT MD simulations were carried out for 40 ns for all the three complex systems using a heat bath coupling time constant of 1 ns.

9.3.5. Binding free energy calculation and per residue energy decomposition

After the MD simulation, the last 5 ns trajectory snapshots (500 frames) of all the three complex systems were subjected to binding free energy decomposition analysis using MM-PBSA.py script [191,192] of AMBER14 suite. MM-PBSA analyses were performed on the three components of each of the complex systems: (i) the protein LMTK3 (ii) ligand (hits) and (iii) the complex (LMTK3-hit compounds). Here, the free energy of the ligand binding is estimated by considering the solvation energies of the interacting molecules in addition to molecular mechanics energies. In general, the binding free energies in condensed phase can be calculated according to the equations that have been described in **Chapter 3** under section 3.5.1.

The interaction between the inhibitor and each residue in the binding site were analysed using the MM-PBSA decomposition process using MM-PBSA.py script of AMBER14 suite. The binding interaction of each ligand-residue pair includes three terms: the van der Waals contribution (ΔE_{vdW}), the electrostatic contribution (ΔE_{ele}) and the solvation

contribution (ΔE_{sol}). All energy components were calculated using the same snapshots as used for free energy calculation.

9.3.6. Potential of mean force (PMF) calculation using Umbrella Sampling simulations method

We calculated the PMF for the three hits with LMTK3 using the Umbrella Sampling (US) simulations [**183**] with the weighted histogram analysis method (WHAM) [**445, 185**]. US simulations were performed in order to describe the unbinding pathway of each hits from its binding site in LMTK3 domain, which may be essential in revealing the inhibitor binding efficiency [**446-448**]. The protocol for calculating PMF has been described in **Chapter 8** under the section 8.3.3.2

9.4. Results and Discussion

9.4.1. Structural validation of LMTK3 domain

We obtained five models of LMTK3 domain from I-TASSER server based on ten different templates using threading program. Based on high C-score value (0.66), the best model was taken. The overall quality of the model was identified by template modelling (TM) score of 0.80 ± 0.09 and root mean deviation (RMSD) of 4.7 ± 3.1 Å. The modelled structure of LMTK3 domain demonstrated the characteristics of protein kinase domain consisting of smaller amino terminal with a combination of one α helix, few anti parallel β sheets and larger carboxy terminal domain with more α helices (**Figure. 9.1**).

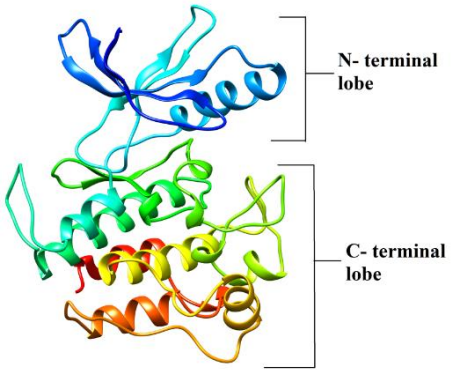

Figure 9.1. *The modelled structure of the kinase domain of LMTK3 obtained from I-TASSER server*

Using ProSA server, the overall quality of the model was validated and the quality index was represented by Z-score of -7.2 (**Figure. 9.2**). Verify-3D server ascertains the accuracy of the predicted secondary structure (3-D) model with its respective residues (1D) by assigning a structural class based on its location and environment. 77.78 % of the residues had an averages 3D-1D score >= 0.2 which confirms the accuracy of the predicted model to near correct to the actual structure. The verify 3D plot is shown in **Figure 9.3.** From the RAMPAGE program, the LMTK3 model was validated by the Ramachandran plot, which shows 87.7 % of the residues are in the favoured regions (243 residues) and 3.6 % of residues are in the disallowed regions (10 residues) as shown in **Figure 9.4**.

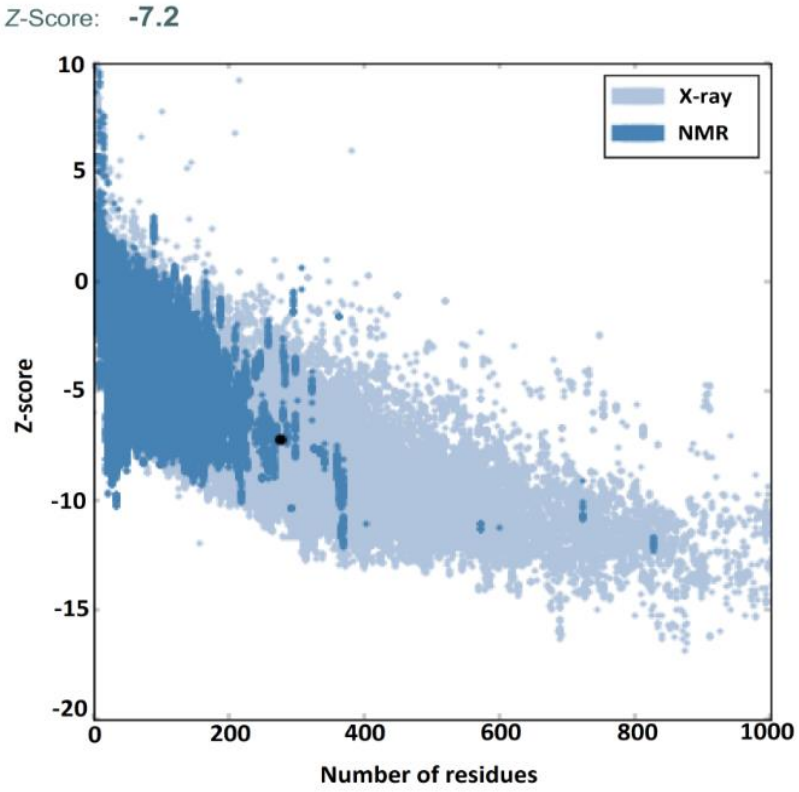

Figure 9.2. *The quality index for the model structure of LMTK3 domain generated by ProSA server. The index value is represented by Z-score*

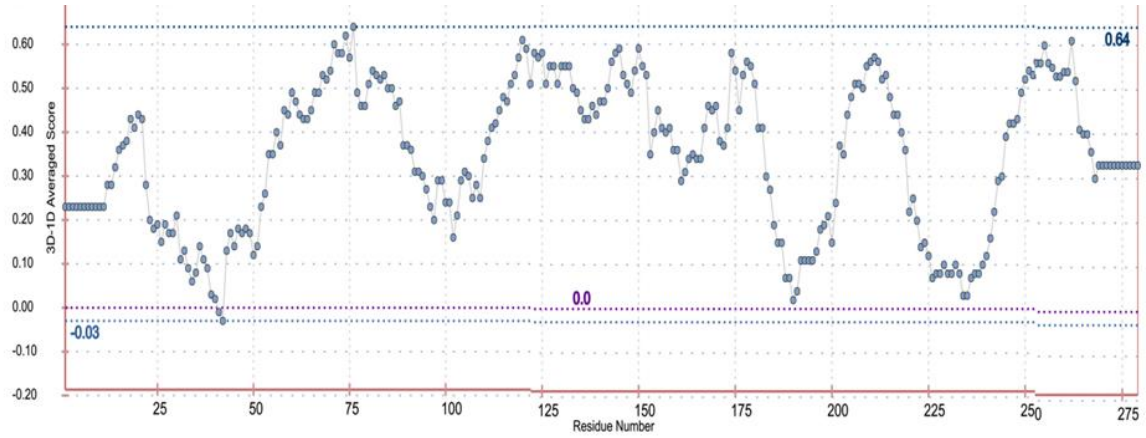

Figure 9.3 *Verify 3D plot of the modelled structure of LMTK3 domain*

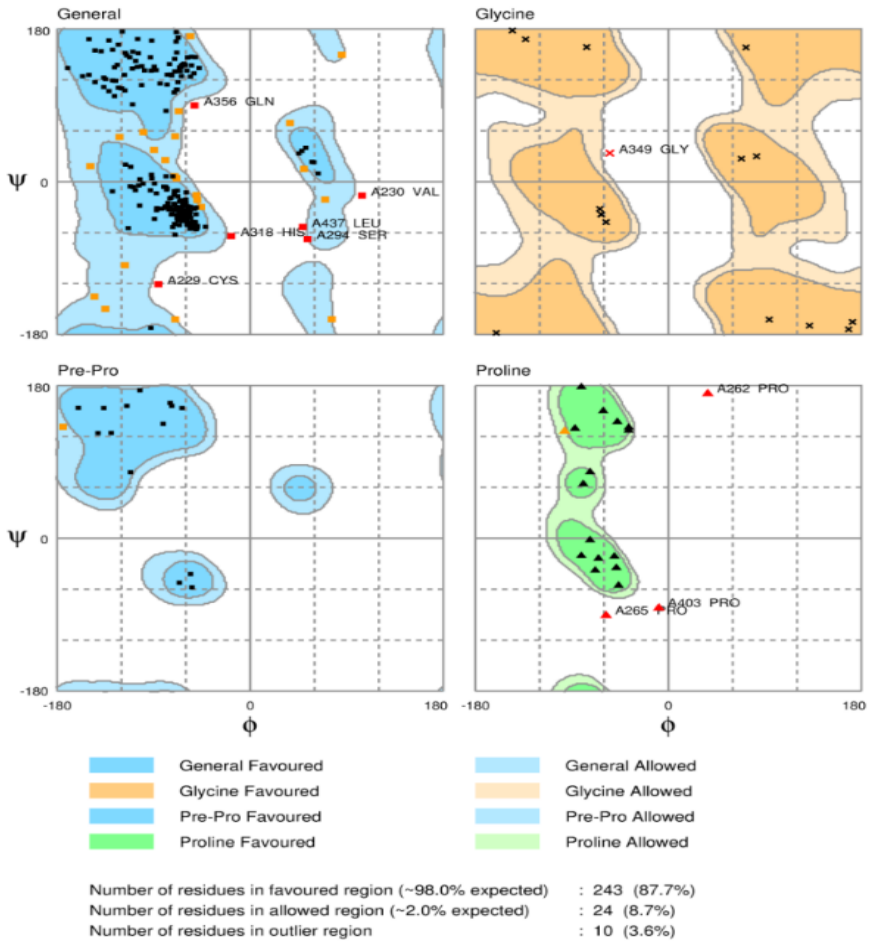

Figure 9.4. *Ramachandran plot of LMTK3 domain: 87.7% of the residues are in most favoured regions, 8.7% of the residues are in allowed region and 3.6% of residues are in disallowed regions*

9.4.2. Database screening and the molecular interaction studies

The Asinex database compounds (more than 300,000 compounds) were initially checked for the redundancy, and then for the druggability using Lipnsiki's rule. The redundant compounds, and the compounds failed during the Lipinski's filter were discarded. High throughput virtual screening was carried out against the modelled LMTK3 domain. Our HTVS results showed the Glide score of the screened compounds were in the range of -5.659 and + 2.689. The top 1000 compounds obtained from the HTVS were further subjected for Glide SP docking and then the refined top 100 compounds from the Glide SP were further subjected for Glide XP docking. The results of the top 10 hits obtained from the Glide XP are represented in **Table 9.1.** And the best top 3 hits among the 10 hits are represented **Table 9.2.**

Table 9.1. Top 10 hits obtained from Glide XP docking

S.No	Compound ID	Docking score	Glide score
1	BDE25665034	-5.639	-5.662
2	BAS12945106	-5.497	-5.497
3	BDE23681078	-5.477	-5.558
4	BDE23027018	-5.451	-5.498
5	BDE26089648	-5.443	-5.517
6	BAS01313675	-5.419	-5.419
7	BDF24025570	-5.386	-5.386
8	BDF24020433	-5.361	-5.361
9	BAS00568142	-5.353	-5.353
10	BDE25464296	-5.299	-5.562

Table 9.2. Glide XP docking scores for top 3 hits and the interacting amino acids of LMTK3 domain

S.No.	Compound ID	Dock score	Glide score	Interacting amino acids
1	BAS12945106	-5.469	-5.469	Arg249,Gln243
2	BDF24025570	-4.996	-4.996	Arg249, Asp313
3	BAS01313675	-4.987	-4.987	Arg249

The 2D structures, database ID, and the chemical names of the top 3 hits are shown in **Figure 9.5**. The E-pharmacophore model was generated from the binding mode of the top hit compound BAS12945106 (based on Glide XP docking score) with LMTK3. Our pharmacophore hypothesis consists of two aromatic rings, a hydrogen bond donor and a hydrogen bond acceptor sites. The developed E-pharmacophore model is illustrated in **Figure 9.6.** These pharmacophoric sites were chosen based on the scores calculated through the Glide XP. The results of the E-pharmacophore analysis are shown in **Table 9.3.**

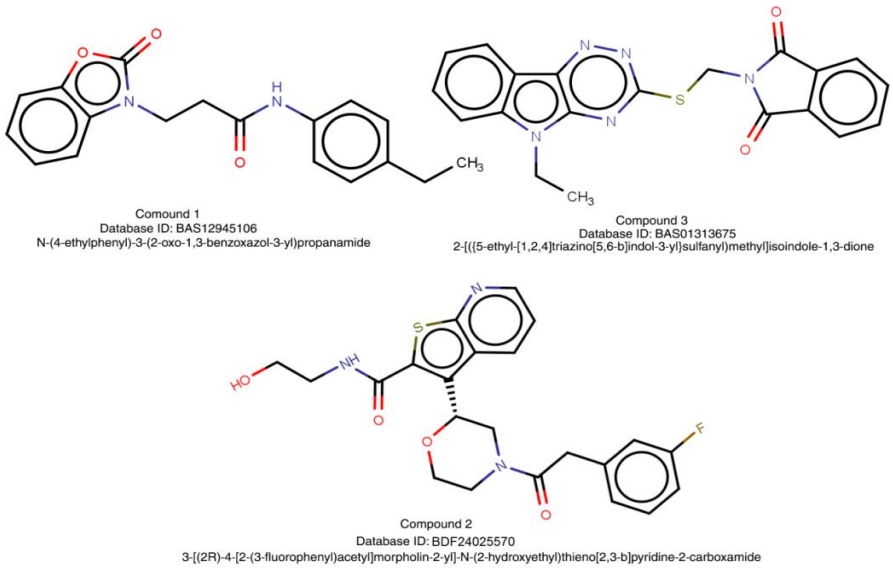

Figure 9.5*. The chemical structures of top three hit compounds with database IDs*

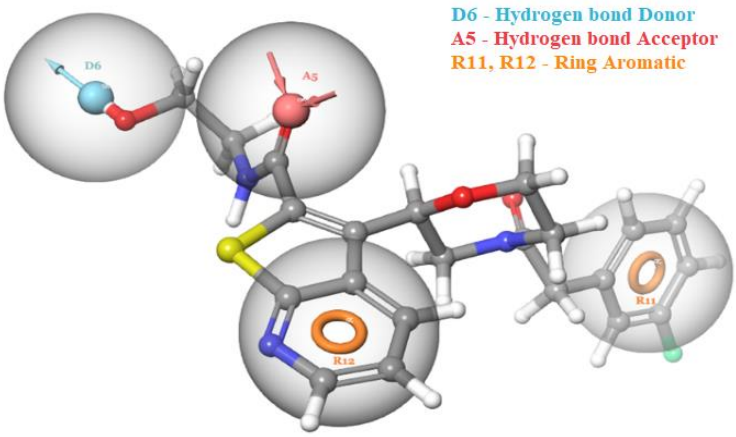

Figure 9.6. *E-pharmacophoric features for LMTK3 inhibitor*

Table 9.3. Features of the E-Pharmacophore Model

Feature label	Type	Score	X	Y	Z	Source
R12	R	-0.7	31.2017	35.5066	34.0291	RingChemscoreHphobe
R11	R	-0.55	40.6484	32.525	31.1979	RingChemscoreHphobe
A5	A	-0.35	40.8003	33.4417	36.7197	HBond
D6	D	-0.35	42.0002	29.5871	39.5911	HBond

9.4.3 Binding mode analysis of three best compounds

The binding modes of the top 3 hits obtained from the Glide XP docking were analyzed. **Figure 9.7** depicts the molecular superimposition of the docked poses of BAS1294510, BDF24025570, and BAS01313675 within the binding site of LMTK3 domain. We remarked all the three hits to be bound at the same site.

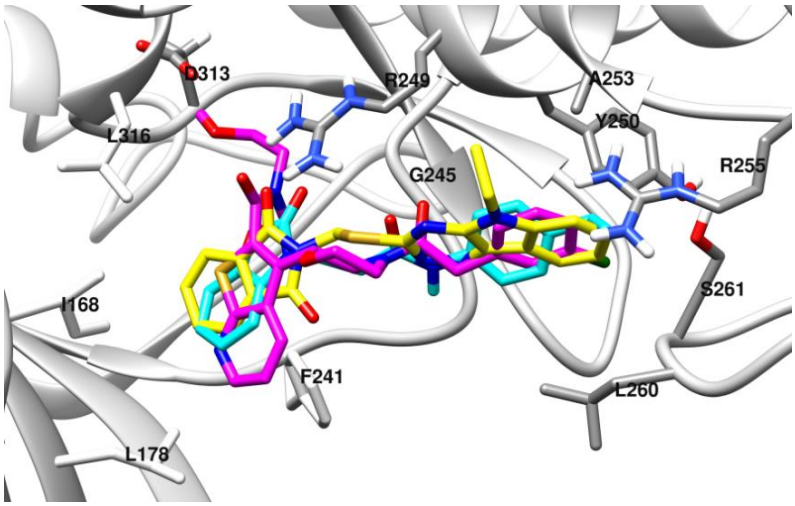

Figure 9.7. *Superimposed binding pose of LMTK3-hit complexes*

Our binding mode analysis revealed that all the three hits were able to form one or more hydrogen bonding interactions with the amino acids of LMTK3 (**Figure 9.8**). The compound BAS12945106 (hit1) with the Glide score of -5.469 formed hydrogen bond (blue colour) interaction with the amino acid Arg249, Gln243 (depicted in brown colour) as shown in **Figure 9.8A.** Compound BDF24025570 (hit2) with the Glide score of -4.996 formed hydrogen bonding interaction with Arg249, and Asp131 as shown in **Figure 9.8B**. Compound BAS01313675 (hit3) with the Glide score of -4.987 formed hydrogen bonding interaction with Arg249 shown in **Figure 9.8C**. At the atomic level hydrogen bonding and hydrophilic interactions between LMTK3 and the three hits were analyzed using Ligplot+ tool [254] as shown in **Figure 9.9.** The summary of the hydrogen bonding interactions was shown in **Table 9.4**.

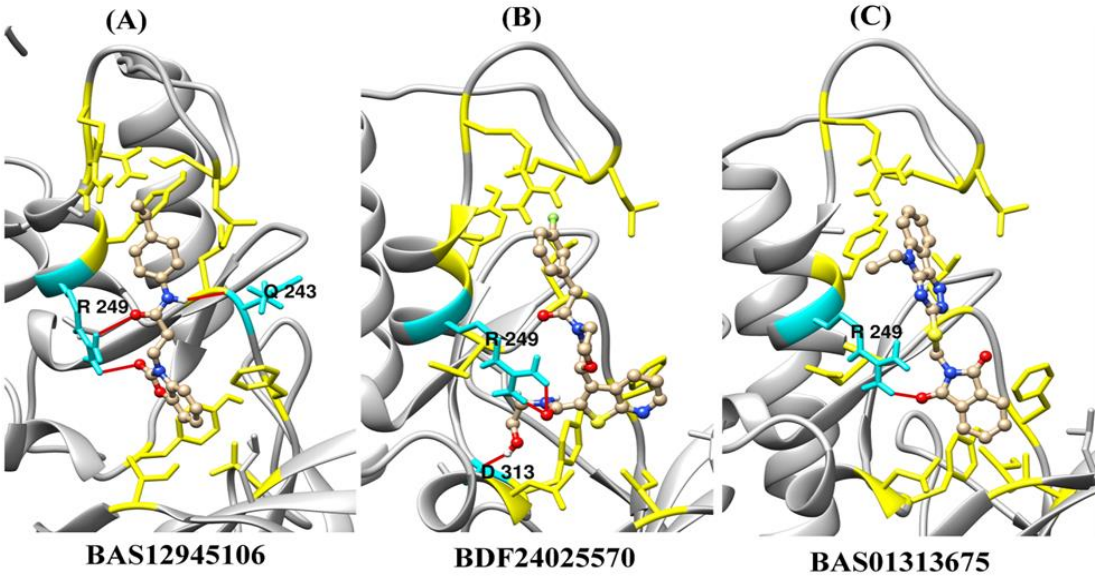

Figure 9.8. *The binding mode of the three hits (BAS1294510, BDF24025570 and BAS01313675) with LMTK3 domain: Residues involved in the formation of hydrogen bonds (depicted in cyan color), hydrogen bonds are in red color, inhibitors are shown in ball and stick form. And the residues involved in hydrophobic interaction with the compounds are depicted in yellow color.*

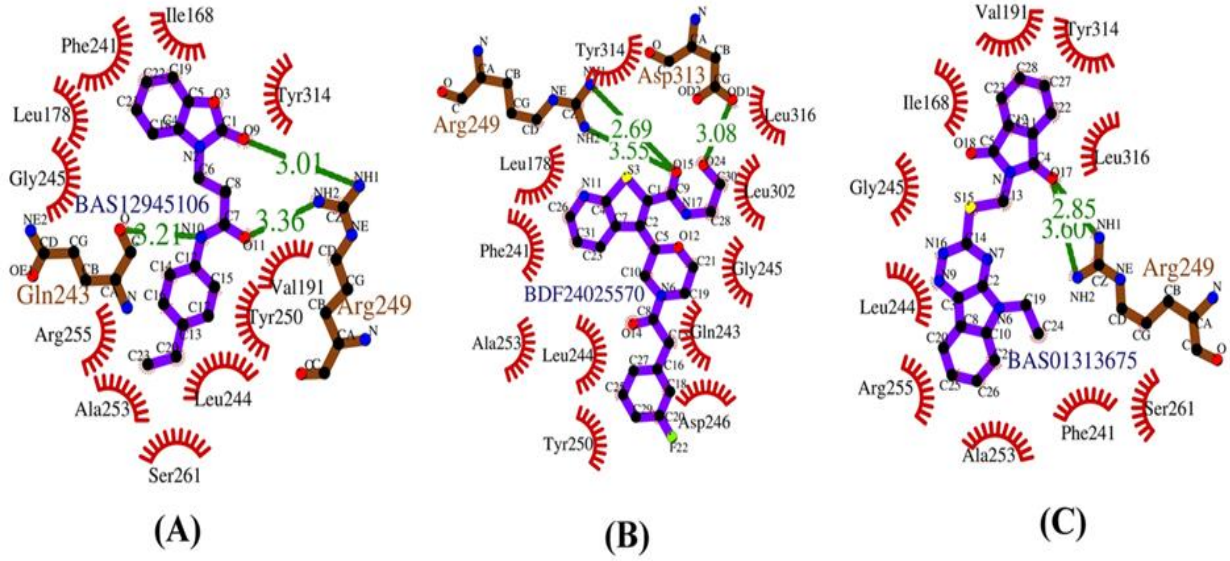

Figure 9.9. *LMTK3 domain complexed with top three hits visualized in Ligplot+: Hydrogen bonds with distance are indicated by green lines between the atoms involved, while hydrophobic contacts are indicated by an arc with spokes radiating towards the ligand atoms they contact.*

Table 9.4. Summary of the Hydrogen bonding interactions of LMTK3 residues with top three hits.

Top three hits	Residue	Protein atom	Ligand atom	Bond length (Å)
BSA12945106	Gln243	O	N	3.21
	Arg249	NH1	O9	3.01
	Arg249	NH2	O11	3.36
BDF24025570	Asp313	OD1	O24	3.08
	Arg249	NH1	O15	2.69
	Arg249	NH2	O15	3.55
BAS01313675	Arg249	NH1	O17	2.85
	Arg249	NH2	O17	3.60

Earlier study [436] had identified the potential inhibitor against ATP site of LMTK3 using the competitive inhibition approach. However, in this study, the identified inhibitors are not binding to the ATP pocket, but were bound to the site distant from ATP binding pocket, may be due to the large size of the inhibitors, unable to reach the ATP binding pocket (**Figure 9.10)**. Earlier studies [467,468] have suggested that inhibitors under Type IV generally binds to the site away from the ATP binding pocket in a distinct allosteric site, and can induce conformational change making the protein inactive. The exact location of the allosteric site of the Type IV kinase inhibitor is not defined specifically, and may bind anywhere on the kinase except for the pocket adjacent to the ATP site (these are considered as Type III inhibitors) [468]. These reports support our study, and thus we can consider our three hits to be the probable allosteric Type IV inhibitor.

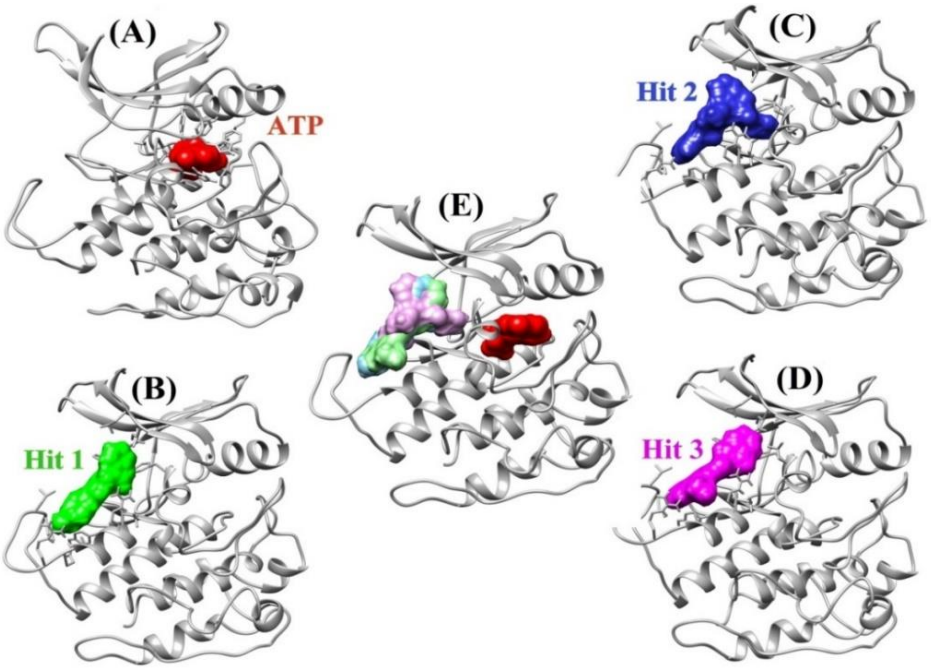

Figure 9.10. *Representation of inhibitors binding to a region distinct from the ATP binding site. Secondary structure shown in grey color, ATP, hit1 hit2, and hit3 depicted in red, green, blue and magenta colour (A-D) respectively. (E) Superimposed LMTK3-hit complexes with LMTK3-ATP complex*

9.4.4. MD trajectory analyses of LMTK3-hit complexes

Molecular dynamics simulations studies of above mentioned three complex systems were performed to further explore LMTK3-hit interactions and their binding mechanism in the dynamic system. To check the thermodynamic stability and consistency of the described systems, different properties like, RMSD, radius of gyration and RMSF, binding free energy calculation, and per-residue decomposition energy were calculated.

To get rationality about the stability of the bound and free LMTK3, RMSD values of the Cα atoms were calculated (**Figure 9.11**). As shown in **Figure. 9.11**, the apo LMTK3 attained stability after 15 ns and held the RMSD value at about 3.5 Å whereas the LMTK3 complex systems attained stability after 5 ns with the RMSD value of around 2.4 Å, indicating the stability of LMTK3 when it is bound to these hits as compared to the ligand-free (apo LMTK3) system. From the RMSD analysis of the complexes, we found the three hits to form stable complexes with LMTK3.

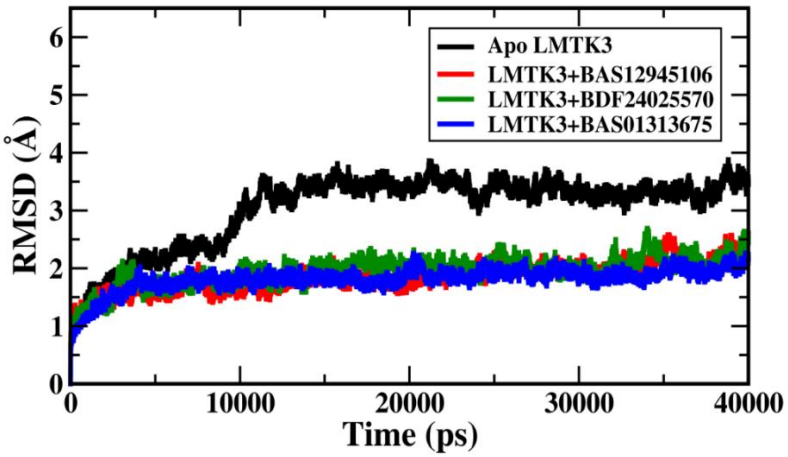

Figure 9.11. *RMSD of apo LMTK3 domain and LMTK3-hit complexes as a function of time.*

We also measured the compactness of LMTK3 and the three LMTK3-hit complexes using the radius of gyration (Rg) analyses (as shown in the **Figure 9.12).** Rg signifies the moment of inertia of atoms from their centre of mass. We can see that Rg value for LMTK3 in complex form takes lower value in comparison with apo-LMTK3. This indicates that LMTK3 is more compact in complex form than apo-form. And also among the three complexes of LMTK3, the LMTK3-hit1 and LMTK3-hit3 complexes (BAS12945106 and BAS01313675) exhibits relatively more compactness than LMTK3-hit2 complex (BDF24025570).

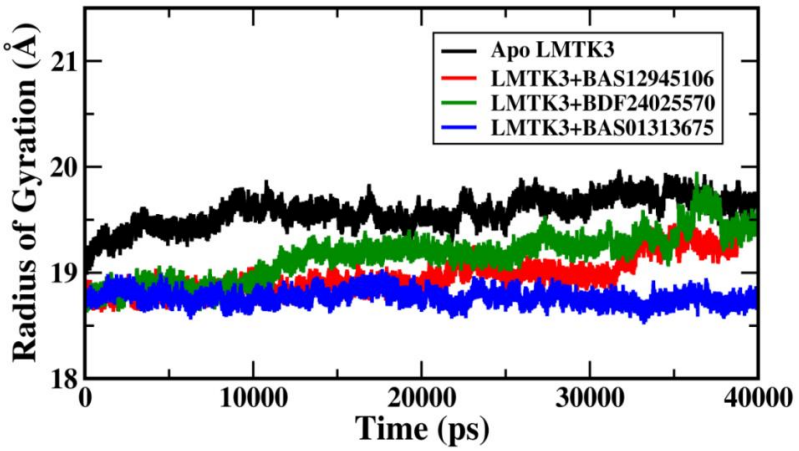

Figure 9.12. *Rg plot of apo LMTK3 domain and LMTK3-hit complexes as a function of time*

The thermodynamic stability of all the LMTK3-hit systems were further characterized by their respective root-mean-square fluctuation (RMSF) values that was done by calculating the Cα atoms fluctuations (around its average position) for each residue. The larger RMSF value indicates more flexibility, while the smaller RMSF values suggest more stable/constrained region. As shown in **Figure 9.13**, the LMTK3 in apo state exhibit more fluctuation, whereas the residues in the complex state that had exhibited crucial interactions with the inhibitors showed less fluctuations while the residues with minimal interactions with inhibitors showed more fluctuation. The RMSF values were larger in the case of apo-LMTK3 and lesser in case of inhibitor bound LMTK3, suggesting that the binding of inhibitor provides more stability to most of the region.

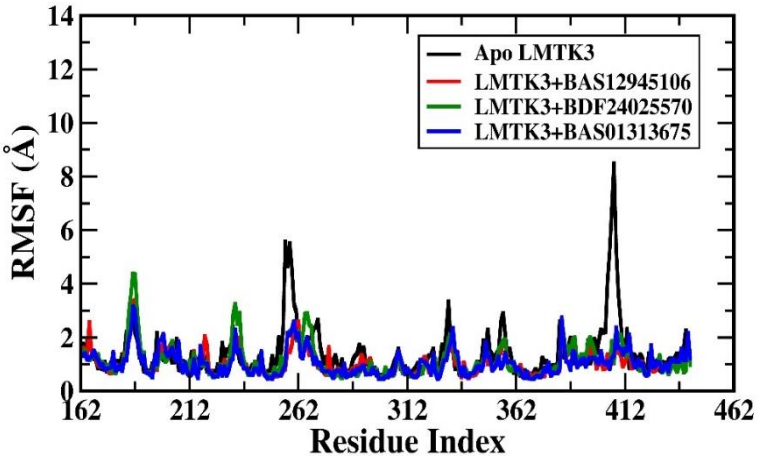

Figure 9.13. *RMSF of apo LMTK3 domain and LMTK3-hit complexes as function of residue index*

9.4.5. MM-PBSA free energy calculation and per residue energy decomposition

The total binding free energies and other component energies of three hits for each LMTK3 complexes were calculated using MM-PBSA method as described in **Table 9.5 (a), (b) and (c)**, respectively. The results show that the value of total binding free energy (ΔG_{total} in kcal mol^{-1}) for BAS12945106-LMTK3, BDF24025570-LMTK3, and BAS01313675 complex are -19.67, -27.39, and -29.57 kcal mol^{-1} respectively, indicating that LMTK3 has similar binding interactions with the inhibitors. From **Table 9.5,** we see van der Waal forces and electrostatic interactions to be the major contributors for the binding of inhibitors with LMTK3.

Table 9.5. MM-PBSA binding free energy calculation for LMTK3-inhibitor complexes

(a) LMTK3-Hit1 (BAS12945106)				
Energy components	**Complex (LMTK3+hit1) kcal mol^{-1}**	**Receptor (LMTK3) kcal mol^{-1}**	**Ligand (hit1) kcal mol^{-1}**	**$\Delta G_{binding}$ kcal mol^{-1} {(complex-(receptor+ligand)}**
VDWAALS	-2322.94	-2287.41	-6.28	-29.24
EEL	-19042.03	-19086.63	50.05	-5.44
E_{PB}	-2593.79	-2593.13	-19.42	18.75
$E_{CAVITY/surf}$	101.44	102.16	3.02	-3.74
G_{gas}	-21364.97	-21374.04	43.76	-34.69
G_{solv}	-2492.35	-2490.97	-16.40	15.01
TOTAL	-23857.33	-23869.01	27.36	**-19.67**
(b) LMTK3-Hit2 (BDF24025570)				
Energy components	**Complex (LMTK3+hit2) kcal mol^{-1}**	**Receptor (LMTK3) kcal mol^{-1}**	**Ligand (hit2) kcal mol^{-1}**	**$\Delta G_{binding}$ kcal mol^{-1} {(complex-(receptor+ligand)}**
VDWAALS	-2322.35	-2282.83	-3.47	-36.05
EEL	-19265.93	-19296.82	46.19	-15.29
E_{PB}	-2397.48	-21.42	-21.42	28.81
$E_{CAVITY/surf}$	97.73	99.31	3.27	-4.85
G_{gas}	-21588.28	-21579.65	42.71	-51.34
G_{solv}	-2299.74	-2305.55	-18.14	23.95
TOTAL	-23888.03	-23885.21	24.57	**-27.39**
(c) LMTK3-Hit3 (BAS01313675)				
Energy components	**Complex (LMTK3+hit3)**	**Receptor (LMTK3) kcal**	**Ligand (hit3) kcal**	**$\Delta G_{binding}$ kcal mol^{-1} {(complex-**

	kcal mol^{-1}	**mol^{-1}**	**mol^{-1}**	**(receptor+ligand)}**
VDWAALS	-2324.93	-2276.09	-5.27	-43.56
EEL	-19190.60	-19217.54	30.80	-3.86
E_{PB}	-2438.27	-2438.11	-23.19	23.02
$E_{CAVITY/surf}$	97.67	99.36	3.47	-5.16
G_{gas}	-21515.54	-21493.64	25.53	-47.42
G_{solv}	-2340.60	-2338.74	-19.71	17.85
TOTAL	-23856.14	-23832.39	5.81	**-29.57**

Further, in order to validate the binding mode and to obtain detailed information on the key residues of the allosteric binding pocket in the complex, the electrostatic, van der Waals, solvation and total contribution of the interacting residues to the binding free energy of the inhibitor-LMTK3 complex were calculated with the MM-PBSA method. The contribution of the selected residues in all the inhibitor-LMTK3 complex in the binding pocket can be clearly seen from the **Table 9.6 a, b,** and **c** and **Figure. 9.14** As shown in **Table 9.5**, the residues Ile168, Leu178, Phe241, Leu244, Tyr250, Gly245, Ala253, Arg255, Ser261, Tyr314, and Leu316 of LMTK3 are involved in hydrophobic interaction with all the three inhibitors, and have favorable total energy contributions, suggesting that these residues participate in binding with inhibitors thus forming stable complex. More importantly, for aforementioned residues, van der Waals interactions play a major role in the total energy contribution for all three inhibitors as shown in **Table 9.6**. The per residue free energy calculation results are consistent with the speculation that the van der Waals interactions contribute more in the binding of inhibitors with LMTK3.

Table 9.6. Decomposition of binding energy on per residues on LMTK3-inhibitor complexes in dynamic system.

(a) Hit 1 (BAS12945106)					
Interacting residues	**ΔE_{vdw} (kcal mol^{-1})**	**ΔE_{ele} (kcal mol^{-1})**	**ΔE_{surf} (kcal mol^{-1})**		**ΔE_{total} (kcal mol^{-1})**
			Polar	**Non-polar**	
Ile168	-0.11	0.05	-0.01	-0.01	-0.07
Leu178	-0.05	-0.01	0.01	-5.73	-0.04
Phe241	-0.33	-0.10	0.18	-0.14	-0.35
Gln243	-0.42	-0.84	1.37	-0.07	0.03
Leu244	-2.23	-0.78	1.49	-0.18	-1.79
Gly245	-0.92	-0.56	0.74	-0.15	-0.91
Arg249	-2.16	-0.59	2.17	-0.35	-0.83
Tyr250	-2.18	-0.53	0.41	-0.15	-2.45
Ala253	-0.73	-0.08	0.89	-0.19	-0.05
Arg255	-0.56	0.32	0.29	-0.08	-0.04
Ser261	-0.68	-0.15	0.66	-0.04	-0.22
Asp313	-0.03	0.38	-0.42	0	-0.04
Tyr314	-0.04	-0.15	0.18	-0.00	-0.08
Leu316	-0.05	-0.04	0.05	-0.00	-0.04
(b) Hit 2 (BDF24025570)					
Interacting residues	**ΔE_{vdw} (kcal mol^{-1})**	**ΔE_{ele} (kcal mol^{-1})**	**ΔE_{surf} (kcal mol^{-1})**		**ΔE_{total} (kcal mol^{-1})**
			Polar	**Non-polar**	
Ile168	-0.65	0.15	-0.08	-0.15	-0.75
Leu178	-0.59	0.21	-0.06	-0.08	-0.53

Phe241	-1.05	-0.02	0.10	-0.20	-1.17
Gln243	-0.84	-1.99	2.24	-0.10	-0.69
Leu244	-2.09	0.47	0.82	-0.10	-0.91
Gly245	-1.19	-1.63	1.05	-0.11	-1.88
Arg249	-2.34	-4.54	6.03	-0.31	-1.16
Tyr250	-1.43	-0.45	0.43	-0.09	-1.54
Ala253	-0.60	-0.07	0.32	-0.12	-0.46
Arg255	-0.63	-0.52	1.37	-0.13	0.09
Ser261	-0.46	-0.02	0.62	-0.09	0.04
Asp313	-0.03	0.69	-0.74	0	-0.07
Tyr314	-0.99	-0.52	0.35	-0.10	-1.26
Leu316	-0.05	-0.04	0.05	-0.00	-0.04
(c) Hit 3 (BAS01313675)					
Interacting residues	**ΔE_{vdw} (kcal mol^{-1})**	**ΔE_{ele} (kcal mol^{-1})**	**ΔE_{surf} (kcal mol^{-1})**		**ΔE_{total} (kcal mol^{-1})**
			Polar	**Non-polar**	
Ile168	-1.41	-0.65	0.95	-0.24	-1.36
Leu178	-0.17	-0.10	0.13	-0.01	-0.14
Phe241	-1.06	-0.16	0.37	-0.22	-1.08
Gln243	-0.84	0.54	0.29	-0.11	-0.13
Leu244	-2.88	-0.62	1.47	-0.26	-2.30
Gly245	-1.64	-1.48	1.29	-0.10	-1.94
Arg249	-3.49	-2.68	5.32	-0.48	-1.33
Tyr250	-1.46	-0.19	0.55	-0.09	-1.21
Ala253	-0.29	0.13	0.01	-0.04	-0.20

Arg255	-0.01	0.08	-0.01	0	0.04
Ser261	-0.09	-0.02	0.03	-0.0002	-0.08
Asp313	-0.06	-1.30	1.38	-4.36E-05	0.02
Tyr314	-1.13	0.21	-0.20	-0.16	-1.29
Leu316	-0.76	0.06	0.24	-0.11	-0.57

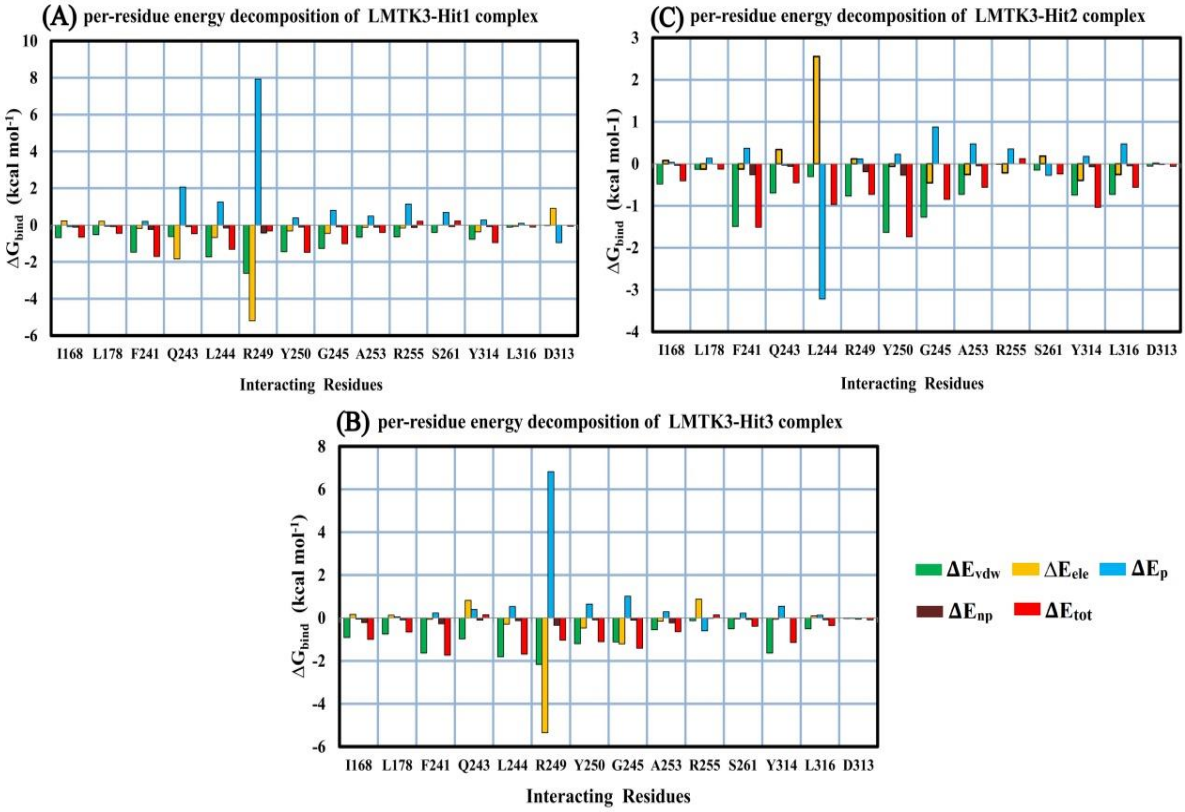

Figure 9.14. *Graphical representation of per residue binding energy decomposition analysis of interacting residues of LMTK3 with (A) hit1 (B) hit2 and (C) hit3*

Among the three hits, hit3 (BAS01313675) showed the highest total binding free energy in the dynamic system, ensuring to be the best E-pharmacophore model. Based on the developed E-pharmacophore model, we hypothesize that the four identified features (two aromatic rings, a hydrogen bond donor and a hydrogen bond acceptor) and their spatial relationships could be essential for a lead compound to potentially inhibit LMTK3 in its allosteric site.

9.4.6. PMF calculations

The equilibrated complex structures of LMTK3-hits were chosen as the initial conformation for the US simulations. The convergence of the PMFs for each system was assured by performing 1 ns US simulations for each window. For instance, different vertical elevation of the PMF (**Figure 9.16**) are observed for the three hits when moves out of the binding pocket of LMTK3 domain. With the increase of the biased potential, ligands move out of the binding pocket. For instance in case of the hit 3 (BAS01313675) (**Figure 9.16**), upgrading of the PMF of reaction coordinates (RCs) are observed when ligand moves out of binding pocket of LMTK3 and finally at 25 Å of RC, the ligand totally dissociate with a high potential energy value of 15 kcal mol^{-1} and the other two hits shows less elevation of the PMF curve, at 25 Å of RC and dissociate with the potential energy value of 2.5 kcal mol^{-1} and 5 kcal mol^{-1} in case of hit 1 and 2 respectively, the hits eventually moves out of the binding pocket. As shown in **Figure 9.16**, the PMF depths from the US simulations of LMTK3-hit complex systems were observed to be much higher in case of hit3 (BAS01313675), which shows a deeper energy potential depth and thus a longer residence time of hit3 in the binding pocket of LMTK3 domain.

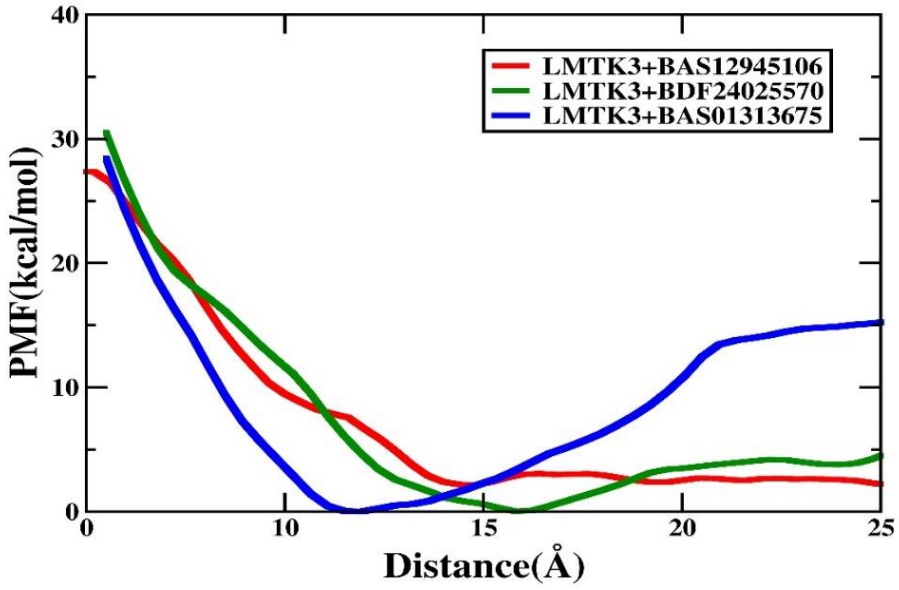

Figure 9.15. *Unbinding process of hits dissociating from the LMTK3 domain*

As shown in **Figure 9.16**, the PMF depths from the US simulations of LMTK3-hit complex systems were observed to be much higher in case of hit3 (BAS01313675), which shows a deeper energy potential depth and thus a longer residence time of hit3 in the binding pocket of LMTK3 domain. The PMF calculation follows the result of MM-PBSA binding energy calculation wherein we see, among the three hits, hit3 has the highest binding free energy and thus high dissociation energy can be seen from the PMF calculation (represented in blue colour). We obtained the order of dissociation energy barrier of our three hits from its binding site of LMTK3 to be BAS12945106 < BDF24025570 < BAS01313675.

9.5. Conclusions

In this study, we have screened the compounds from Asinex database against LMTK3 domain using Schrodinger Drug Discovery Suite. The hierarchical structure based virtual screening protocol, including HTVS, standard precision (SP), and extra precision (XP) was performed to the Asinex database against LMTK3. Based on the high Glide XP score, we selected the top three hits (BAS12945106, BDF24025570, BAS01313675) containing pharmacophoric features. The three hits have shown hydrogen bonding and non-bonding interactions with LMTK3 in the non-ATP binding site. The complexes of LMTK3 with the three hits were found to be stable from the RMSD, Rg analysis and MM-PBSA binding free energy calculations. In addition, from the per-residue energy decomposition analysis, we have seen that van der Waals interactions contribute more in the binding of three hits to the LMTK3. From PMF profile we noticed, among the three hits, hit2 (BAS01313675) to have higher dissociation energy barriers. Based on the Glide XP docking score of the top three hits and from their binding modes, an energy optimized (E) pharmacophore model was generated. Our pharmacophore hypothesis consists of two aromatic rings, a hydrogen bond donor and a hydrogen bond acceptor sites. These pharmacophoric features may be helpful in the development of new potential inhibitors to target LMTK3 for effective breast cancer therapeutics.